7. Turbulent Flows

7.1 Fundamentals of Turbulent Flows

When a viscous fluid flows through long straight tubes at reasonably high speeds, the Hagen–Poiseuille law, according to which the pressure drop is linearly proportional to the volume of fluid flowing through the pipe, is replaced by another law, in which the pressure drop is significantly greater, and almost proportional to the square of the volume flow rate of fluid. At the same time it is found that the flow field, which is smooth and straight (or *laminar*) in the Hagen–Poiseuille regime, becomes at higher velocities full of irregular eddying motions (or *turbulent*). This may be seen clearly in the case of a fluid flowing through glass tubes if a dye is introduced through a small injector at the inlet (Figures 7.1, 4.53). The colored filament is straight and smooth for low speeds but breaks off and disperses almost uniformly when turbulence develops. As a second example, consider a jet of water that emerges from a circular orifice into a tank of still water. At very low speeds of the fluid the

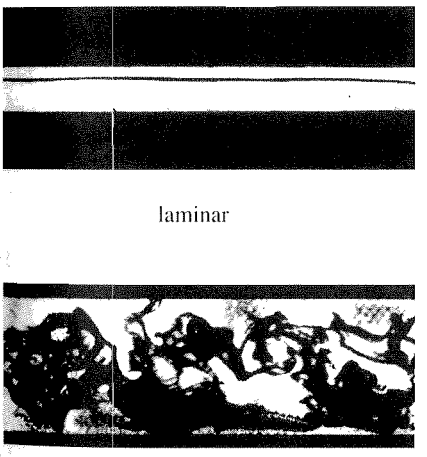

Fig. 7.1 Laminar and turbulent pipe flow

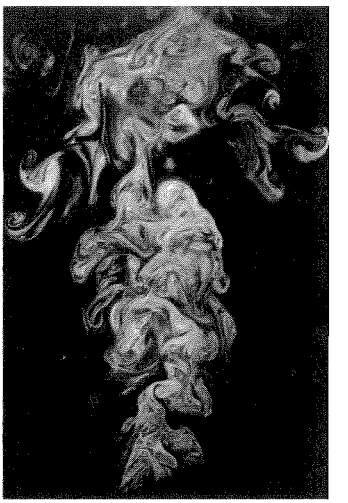

Fig. 7.2 Turbulent water jet

jet is smooth and steady. For higher speeds, it develops swirls of various sizes amidst avalanches of complexity (Figure 7.2).

The two figures, being static, do not do justice to the dynamical interactions occurring within the flow. Observation suggests that parcels of fluid get stretched, folded, and tilted as they evolve, in turn losing shape by agglomeration and breakup, while new ones are constantly being created. This evolution and development of the flow does not repeat itself in full detail. Together, these features have a profound influence on the ability of the turbulent flow to transport heat, mass, and momentum. Under suitable conditions, turbulence occurs in such varied flow configurations as boundary layers, wakes behind objects, thermal convection, and geophysical and astrophysical flows. The turbulence in each of these contexts is different in detail but similar in its function.

As a practical matter, turbulence plays an important role in technology and control phenomena such as weather and climate that have a large effect on human activities. Without turbulence, the mixing of air and fuel in an automobile engine would not occur on useful time scales. The transport and dispersion of heat, pollutants, and momentum in the atmosphere and oceans would be far weaker. In short, life as we know it would not be possible on Earth. Turbulence also has undesirable consequences. It increases energy consumption of pipelines, aircraft, ships, and automobiles and is an aspect to be reckoned with in air-travel safety, and it distorts the propagation of electromagnetic signals, and so forth. A major goal of a turbulence practitioner is the prediction and control of the effects of turbulence in various applications such as industrial mixers and burners, nuclear reactors, aircraft intakes, around ships, and inside of rocket nozzles. A major goal of a physicist working in turbulence is to understand the dynamical origin of this complexity, describe and quantify its features, and understand the universal properties embedded in features that are specific to a flow. A larger goal is to understand whether the statistical complexity of turbulence is shared in a serious way by other phenomena such as granular flows, fractures, and earthquakes.

In summary, then, turbulence is a rich problem both as a paradigm of spatiotemporal complexity and as a matter of practical importance. There are three major aspects to be considered: the origin of turbulence, the phenomena of flows in which turbulence is already developed, and the control of turbulence in a given situation. We will be concerned primarily with the second feature here, though brief remarks follow on the onset of turbulence.

7.2 Onset of Turbulence

During the last 120 years or so a great deal of ingenuity has been expended, on both mathematical and experimental fronts, on answering the question of how turbulence arises, and a reasonable picture has emerged, at least in some instances (see Section 4.2.4). Qualitatively, the transition from the laminar to the turbulent state occurs if the momentum exchange by molecular transport cannot compete sufficiently effectively with the transport due to macroscopic fluctuations in flow velocity. Making use of the ideas of dynamic similarity, *O. Reynolds* (1883, 1894) argued that the transition from the laminar to the turbulent state occurs when a nondimensional parameter, now bearing his name, exceeds a certain critical value. The Reynolds number (4.51) is defined as Ul/ν, where U is a characteristic velocity of the flow, l its characteristic size, and ν the kinematic viscosity of the fluid.

The situation is more complex than was originally presumed by Reynolds. For instance, the numerical value of the critical Reynolds number depends on the flow and a number of other factors such as the initial disturbance level (besides the obvious dependence on the precise definitions selected for the velocity and length scales). The notion that flows are laminar and stable up to a certain critical Reynolds number, becoming turbulent thereafter, turns out to be somewhat naive in practice.

7.2.1 Linear Stability

A generic case of instability to consider in a carefully prepared experiment is one in which the perturbations are small. This idea has prompted a vast development of linear stability theory, the theory that calculates the Reynolds number at which laminar motion becomes unstable to small perturbations. Starting with *Lord Rayleigh* in the 1880s, *O. Reynolds* (1883), *W.M.F. Orr* (1907), *A. Sommerfeld* (1908), *G.I. Taylor* (1923), *W. Heisenberg* (1924), *C.C. Lin* (1955), *S. Chandrasekhar* (1961), and others (see, for example, *P.G. Drazin, W.H. Reid* (1981) for details) have made lasting contributions to the subject.

Since the instabilities grow only at relatively high Reynolds numbers (or equivalently, small viscosities), it appears reasonable at first to treat the problem as essentially inviscid. Indeed, inviscid instability is often able to explain certain observations concerning the behavior of fluids with finite viscosity. This turns out to be the case particularly for flows for which the maximum vorticity occurs within the bulk of the fluid instead of on the boundaries. An excellent example is the so-called mixing layer, the flow formed when two parallel streams with different velocities come together (see *A. Michalke* (1970)).

Inviscid instability yields implausible answers for certain other flows. For instance, the theory yields the result that the flow between two parallel plates, one of which is stationary while the other moves with finite velocity, called plane Couette flow, is stable at all Reynolds numbers. Experiments, on the other hand, show that the flow does indeed become unstable at some finite Reynolds number on the order of a thousand (when based on the velocity of the moving plate and the distance between the plates). This phenomenon is puzzling at first sight because if a flow is stable in the absence of viscosity, the additional damping provided by viscosity may be thought reasonably to

make it even more stable, not less so. However, viscosity plays a subtle role, as explained by *W. Tollmien* (1929), and more fully by *C.C. Lin* (1955), and can promote instability (see *P.G. Drazin, W.H. Reid* (1981)).

These issues are best explained for the case of a boundary layer on a thin flat plate, for which extensive literature is available (see Section 4.2.4). This is an important flow in practice because it will be seen that turbulence often arises within a boundary layer. To study the initial growth of the perturbation in the boundary layer of a viscous fluid, *W.M.F. Orr* (1907) and *A. Sommerfeld* (1908) derived from the Navier–Stokes equations a linear differential equation (4.73) that is now named after them. The solutions of this equation are of the form shown in Figure 4.58. Inside the neutral curve ($\omega_i = 0$), the two-dimensional wave perturbations are unstable ($\omega_i > 0$), and outside, they are stable ($\omega_i < 0$). In regions of instability, the perturbations grow exponentially (with time if they are spatially homogeneous, or with space if introduced at some point in space and allowed to grow as they propagate, or in both space and time if the perturbations are in the form of a wave packet).

Further investigation shows that a second characteristic layer is formed at the position in the flow where the velocity of the main flow is the same as the phase velocity of the oscillation. In the absence of friction this would lead to singularities in the motion of fluid particles, since they are subject to the same pressure gradient for a very long time. However, if viscosity is postulated in this second layer also, then the disturbance is free from singularities. With the presence of viscosity, the phase displacement of longitudinal motion produces a damping effect, which, in conjunction with the amplification due to the secondary boundary layer, gives a critical value for the Reynolds number. Here we have only hinted at the basic physics, but it was the notable achievement of *W. Tollmien* (1929) to carry out the calculation needed to compute the critical Reynolds number.

There are other flows for which the linear stability theory gives excellent results for the loss of stability. This loss of stability is often expressed in terms of nondimensional parameters that are related to a suitably defined Reynolds number. For instance, the theory (*H. Oertel Jr. and J. Delfs* (1996), Chapter 8) predicts rather well the so-called Taylor number at which the flow between concentrically rotating cylinders loses stability and begins to form torroidal vortices. The Taylor number is the square of the Reynolds number based on the angular velocity of the rotating cylinder, the gap between the two cylinders, and the viscosity. The theory similarly predicts well the so-called Rayleigh number, Ra, at which the heat transfer changes from a steady conductive mode to a structured form involving hexagonal or roll patterns. The Rayleigh number is a measure of the ratio of the effect of buoyancy, which tends to accelerate a fluid parcel against gravity, to the viscous and diffusive effects that tend to slow it down. For the fluid between a pair of infinitely extended horizontal plates, with the bottom plate heated and the top plate cooled, the heat transport ceases to be purely conductive at $\mathrm{Ra} = 1708$ (see

Section 8.2.1). In engineering literature on so-called free convection problems, the Grashof number $\mathrm{Gr} = \mathrm{RaPr}$ is often used, where the Prandtl number is $\mathrm{Pr} = \nu/\kappa$ (see Section 9.2), κ being the thermal diffusivity of the fluid.

In a broad class of flows, a few of which were just mentioned, the loss of linear stability of the laminar state is a significant first step in the formation of turbulence. There is more detail to be found in Chapter 8. The next step in the process of complexity is the nonlinear stage, at which the perturbations have grown to sufficiently large amplitude at which they begin to interact with the mean flow and cease to grow exponentially as a result of this interaction. This is discussed below briefly.

7.2.2 Nonlinear Stability

Fascinating advances have been made with respect to successive instabilities potentially leading to turbulence. *L.D. Landau* proposed a quasi-periodic route to turbulence (see *L.D. Landau, E.M. Lifschitz* (1991)) in which successive instabilities occur at ever faster rates and culminate in turbulence at their accumulation point. Other possibilities such as the few-step route (*D. Ruelle, F. Takens* (1971)) and the period-doubling route (e.g., *M.J. Feigenbaum* (1978)) have been proposed for the generation of temporal complexity (or chaos) in a variety of nonlinear systems. Indeed, these scenarios have been observed in many nonlinear systems including fluid flows (and are thus believed to be universal in scope), but the appearance of turbulence is an issue of both temporal and spatial complexity. Here, progress is attained more or less on a case-by-case basis, although some generality of concepts does exist. In particular, the route to turbulence is not unique, because, among other things, the process is not merely one of successive instabilities but also one of flow receptivity to a variety of background fluctuations that are invariably present. For instance, for the flat plate boundary layer, unless the disturbance level is carefully controlled, the process of transition may be bypassed altogether, and pointlike disturbances may evolve into three-dimensional wave

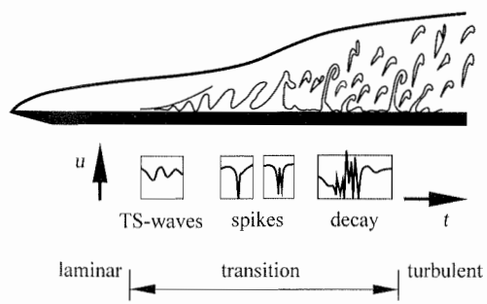

Fig. 7.3. Transition in the plate boundary layer, *M. Nishioka et al.* 1990

packets that grow quickly into spots of turbulence. These spots coalesce to form turbulence as we know it.

For the boundary layer, when the background noise level and initial conditions are carefully controlled, a variety of details can be reproduced, and the following sequence of events occurs (Figure 4.56). Once the modes of primary instability, known as the Tollmien–Schlichting waves, grow to finite amplitudes, the flow develops spanwise variations. These spanwise variations appear rather slowly in wind tunnels, and are better studied when induced artificially, as was done by *P.S. Klebanoff et al.* (1962), who attached small strips of tape at equal intervals across the plate. Their measurements revealed the appearance of counterrotating vortices, and the development of definite *peaks* and *valleys* in the fluctuation velocity. As spanwise variation intensifies, a thin layer of high shear appears, especially at the peak, consistent with the observations of *L.S.G. Kovasznay et al.* (1962). *J.T. Stuart* (1963) has shown that the convection and vortex-stretching in the presence of large spanwise variations produce small layers of high intensity, resembling those observed experimentally. These layers possess inflection points and are inviscidly unstable, thus leading to further high-frequency modes and the formation of new vorticity in both longitudinal and spanwise directions. The passage of the vortex structures results in spikes in velocity signals, as seen in the extensive studies of *M. Nishioka et al.* (1990) for the case of a two-dimensional channel (Figure 7.3). Near where the spikes occur, spots of turbulence are born. Turbulent spots (*H.W. Emmons* (1951)) have a well-defined shape within which the fluid is in nearly turbulent motion, and are surrounded by essentially laminar flow. The spots grow as they propagate and merge with other spots to become fully developed turbulent flow. The growth rate of isolated spots is proportional to the square root of the difference between the Reynolds number of the flow and the Reynolds number at which spots are born.

For a more detailed description of laminar–turbulent transition in the boundary layer, see *R. Narasimha* (1985).

7.2.3 Nonnormal Stability

The combination of stability theory and experiment has been able to advance our understanding of the origin of turbulence in certain broad classes of flows illustrated above. However, there are other circumstances for which linear stability is an unsuitable starting point for understanding the onset of turbulence. In those instances the onset of turbulence is sudden, and a fundamentally different sequence of events is involved. In particular, the many scales of turbulence appear more or less at the same time. Flow through pipes is an excellent example of this kind of transition. Typically, flows of this kind are stable to all linear perturbations, and one of their strong characteristics is that the transition has no reproducible *critical* Reynolds number, as would be characteristic of linear instability. The Reynolds number at which the transition to turbulence occurs depends on the type, form, and magnitude of

the disturbance. For the onset of turbulence, the initial disturbance and the Reynolds number need to be large enough, and play complementary roles, where a smaller disturbance level is needed at larger Reynolds numbers, and vice versa. If the pipe is joined to a smooth-walled vessel by a sharp edge, the critical Reynolds number is about 2800. If the inlet is well rounded and the flow there is prepared to be relatively free of disturbances, transition values as high as 10^5 can be observed. If the inflow is very irregular, it may fall to about 2300 (see Section 4.2.4). In fact, in the last case, the transition Reynolds number is representative of the conditions at which large initial disturbances *just* manage to regenerate continually. In contrast to pipe flow, which is linearly stable for all Reynolds numbers, channel flow is expected to become linearly unstable at a finite critical Reynolds number of 5772 (*C.C. Lin* (1945), *S.A. Orszag* (1971)). However, experiments show that the transition does not usually wait until that Reynolds number is reached, but occurs at lower Reynolds numbers.

The mechanism of transition in these cases is called subcritical because it occurs below the linear stability value. *W.M.F. Orr* (1907) knew that linear disturbances of a shear flow could grow for some time even if they are stable (since the concept of stability is related to the asymptotic growth of perturbations). Many later authors have expanded on this theme (for a summary see *S. Grossmann* (2000)).

Figure 7.4 shows a schematic plot of subcritical transition. With increasing initial disturbance amplitudes A the transition to turbulence occurs at smaller Reynolds numbers Re. The transition line should be interpreted as the envelope of all stability lines for possible types of disturbances.

It is now clear that the nonnormality of eigenfunctions of the linear operator for the perturbation equation is the essential property responsible for the transient growth of disturbances. This, together with the proper action of the nonlinear interactions between finite disturbances of sufficient amplitude, leads to the onset of turbulence. The nonnormality of the linear dynamics quite generally implies a bunching of the eigendirections. Those disturbances that fit into the bundle decay with time, while those that do not do so first grow algebraically at a rate that depends on the nonnormality and the Reynolds number. Only after this transient increase do they decay.

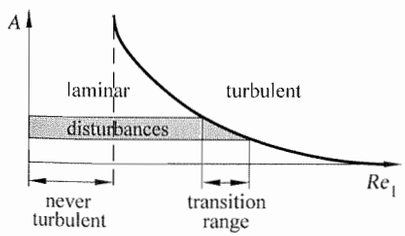

Fig. 7.4. Subcritical transition

But if there is sufficient transient amplification, the nonlinearity, which can no longer be neglected, drastically modifies the dynamics, and the appearance of an irregularly fluctuating velocity field can be expected.

7.3 Developed Turbulence

7.3.1 The Notion of a Mixing Length

The two flows with which we started this chapter are examples of developed turbulence. In practice, we do not need to know all the details of turbulent flows, but we wish to obtain answers to questions such as, How fast does a jet grow on the average? How much power is required to pump a fluid at a certain rate through a pipe? How much power is required to fly an aircraft? How much fuel is consumed in providing a required amount of thermal energy in a combustion chamber? It is useful for these purposes to decompose the velocity into mean and fluctuating parts (called *Reynolds decomposition* after Osborne Reynolds (4.63); see Section 4.2.4), and to obtain suitable equations for the mean part. This can be done by substituting the Reynolds decomposition into the Navier–Stokes equations and averaging them. This operation yields new equations (the so-called *Reynolds* equations, see Section 5.2.2) that look similar to the original equations except that a new stress term appears in addition to the viscous stress. Mathematically, the source of this new term is the nonlinearity of the advection term in the Navier–Stokes equations. Physically, turbulent fluctuations gives rise, on average, to increased momentum transport by transporting momentum from place to place in the flow. The new shear stress (called the *Reynolds shear stress*) has the form $\tau = -\rho\overline{u'v'}$, where u', v' are deviations of the velocity components from their average values $\overline{u}$ and $\overline{v}$, respectively, and the overline indicates the average over time. In order to solve the Reynolds equations and obtain formulas of practical use, we must express τ in terms of other quantities related to the mean velocity. The situation, called the *closure problem*, is analogous to that in kinetic theory in which the momentum transport of molecular theory is seen as a macroscopic viscosity, which must be prescribed. However, viscosity is a property of a fluid that can be measured once and for all. Such simplicity does not exist in turbulence for reasons that we shall mention presently, and so a variety of methods has been devised to express the Reynolds stresses in relation to the distribution of the mean velocity. The methods developed have varying levels of success but are not universally applicable to all turbulent flows. Approaches vary from the application of sophisticated statistical mechanical principles or hypotheses, whose physical content is not immediately apparent, to the use of more or less transparent physical ideas, which cannot always be justified.

The simplest intuitive physical picture of *L. Prandtl* has historically allowed us to make some progress by assuming that fluid parcels (or *eddies*) of

a certain size transport momentum through the fluid by means of their seemingly random motion. If so, it is appropriate to associate one length scale with the "diameter" of these eddies, and another for the distance through which they remain intact as they propagate relative to the rest of the fluid. We cannot say a priori that these two lengths are the same, but we expect that they might be proportional to each other. We now assume that the flow is such that the mean velocity varies in a direction at right angles to the streamlines (as in pipe flows). If, as shown in Figure 4.62, a fluid parcel is displaced from a position y where the mean velocity is $\overline{u}(y)$ by a distance l in a direction transverse to the flow, the difference between its old and new velocities is $\overline{u}(y+l) - \overline{u}(y)$. As a first approximation, we may write this as $l\partial\overline{u}/\partial y$. This gives an estimate of the order of magnitude of the fluctuation u'. The value of v' is found from the assumption that two parcels of fluid, which enter the layer in question from opposite sides and subsequently move on after each other, approach or recede from one another with relative velocity $2l\partial\overline{u}/\partial y$. This gives rise to transverse velocities of the same order of magnitude as u'. Thus, in forming the average value $\overline{u'v'}$, we have still to consider the signs of the corresponding u and v components. It is easy to see, however, that in crossing a control surface parallel to the boundary, the fluid particles moving away from the boundary are relatively slow compared to those moving toward the boundary. Therefore, in general, negative values of u' are associated with positive values of v', and positive values of u' with negative values of v'. Thus the product $u'v'$ tends to be negative in both cases, and the new shearing stress is positive and of order $\rho(l\partial\overline{u}/\partial y)^2$. If we arbitrarily take the unknown factor of proportionality as unity, we merely make a slight change in the meaning of l. To make the formula accurately express the fact that a positive shearing stress corresponds to positive values of $\partial\overline{u}/\partial y$ and a negative shearing stress to negative values of $\partial\overline{u}/\partial y$, we must write

$$\tau' = \rho\, l^2 \left|\frac{\partial\overline{u}}{\partial y}\right| \frac{\partial\overline{u}}{\partial y}. \tag{7.1}$$

From this approximate expression, we infer that the Reynolds stresses due to turbulent motion are proportional to the square of velocity increments, leading to the notion that fluid resistance varies roughly as the square of the velocity in a turbulent flow. The length l, called *Prandtl's mixing length*, is not unlike the molecular mean free path $\overline{\lambda}$ in the kinetic theory of gases. In the latter, the transfer of momentum due to motion of molecules is discussed in a way similar to our present account of the transfer of momentum by the large-scale motion of fluid parcels. As in the present case, the deviation from the mean velocity of particles, moving upward or downward, is given by $u' = \pm\overline{\lambda}\,\partial\overline{u}/\partial y$. The transverse velocity v', however, is not proportional to u', but is equal to the molecular velocity, effectively a constant. Thus, the shearing stresses due to molecular motion (the viscous stresses) are linearly proportional to $\partial\overline{u}/\partial y$. In gases, the mean free path $\overline{\lambda}$ is inversely proportional

to the density ρ, so that the factor $\rho\overline{\lambda}$ present in the definition of viscosity is independent of the density.

If we insert $\mu_t = \rho l^2|\partial\overline{u}/\partial y|$ into the above equation, we obtain the equation $\tau' = \mu_t \partial\overline{u}/\partial y$. This is of the same type as the equation for the viscous shearing stress $\tau = \mu\partial u/\partial y$, and μ_t has the dimensions of viscosity. Unlike the molecular viscosity coefficient, however, μ_t, known as the *eddy viscosity coefficient*, depends on the details of the flow and its Reynolds number. Another important difference from ordinary viscosity is that μ_t is not a unique property of the fluid and varies from point to point in the flow. For example, it tends to zero as the boundary wall is approached. In practice, these attributes limit the usefulness of the concept of eddy viscosity. Neither is the notion as compelling as in the molecular case, where there is a large separation of scales between the molecular mean free path and the scale characterizing the mean flow gradient. Indeed, in turbulence, the mixing length is often not a negligibly small fraction of the flow size. In spite of these basic limitations, the notion of mixing length is qualitatively ingrained even in sophisticated theories of turbulence.

7.3.2 Turbulent Mixing

The effects of turbulence include not only increased momentum transport, but also the transfer by convection of all the properties of moving matter (heat content, quantity of admixed matter, etc.). With some exceptions, the transport of a given property will occur, on average, from regions rich in that property to those that are lacking in that property. In the case of temperature differences, this means some type of turbulent heat conduction; in the case of differences in concentration, a type of turbulent diffusion will result. Thus, since the quantity of heat contained in unit mass of a fluid is c_pT, where T is the temperature and c_p the specific heat at constant pressure, the net quantity of heat flowing across unit area per unit time is given by

$$Q = -c_p\kappa_t\frac{\partial\overline{T}}{\partial y} = -c_p\rho l^2\left|\frac{\partial\overline{u}}{\partial y}\right|\frac{\partial\overline{T}}{\partial y}. \tag{7.2}$$

That is, $c_p\kappa_t$ is the thermal diffusivity ($\lambda_t = c_p\cdot\rho\kappa_t$). In the case of a chemical or mechanical admixture of concentration c, the mass of admixed substance transferred across unit area in unit time is given by

$$M = -\rho D_t\frac{\partial\overline{c}}{\partial y}. \tag{7.3}$$

There remains the question of whether κ_t and D_t agree numerically with $\nu_t = \mu_t/\rho$, considering that the mechanism of propagation of a property of matter, or of an admixed substance, is not quite the same as that of transfer of momentum. The ratios ν_t/κ_t and ν_t/D_t are known as the turbulent Prandtl number and turbulent Schmidt number, respectively (see Section 9.4). Their numerical values depend on whether one is considering turbulence near a solid boundary, or in regions away from it (the so-called free shear flow).

This last-mentioned difference is connected with differences in the eddy structure between the two classes of flows. Loosely speaking, eddies with their axes parallel to the direction of flow predominate near a solid boundary, whereas the eddies with their axes at right angles to the flow direction predominate in free shear flows. Eddies of the first kind make no contribution to the transport of momentum, whereas eddies of the second kind make a very considerable contribution. Therefore, the distributions of mean velocity and of mean temperature or concentration exhibit marked differences. That the heat exchange is more dominant than the momentum exchange in the case of free turbulence has also been shown by experiments on the smoothing out of temperature and velocity distributions in the rear of lattices of heated rods, where the temperature differences vanished much more rapidly than the velocity differences.

In general, since turbulent transport and mixing depend largely on the motion of parcels of fluid, one may imagine that they become essentially independent of molecular properties. It is in fact true that the momentum transport far away from the wall becomes asymptotically independent of the fluid viscosity. The situation very near the wall is that the viscosity always plays an important role because turbulent fluctuations are small there. Turbulent mixing of admixtures does seem to retain some weak dependence on the molecular Prandtl or Schmidt number (as appropriate). This seems to be the result of the fact that parcels moving through the turbulent background develop transient boundary layers on their front side, and reintroduce the molecular Prandtl or Schmidt number effects indirectly.

7.3.3 Energy Relations in Turbulent Flows

Work is done on a fluid element by the Reynolds stresses and the corresponding pressure differences. This work serves to maintain the turbulent motion within the element. In the very simple picture considered above, the work done on unit volume per second is $\tau'\partial\overline{u}/\partial y$. This work enables the eddying motion to maintain itself against the resistance that it encounters in its motion. The initial forward motion of the individual eddy, relative to its surroundings, is itself a turbulent motion, which, if its Reynolds number is sufficiently high, gives rise to a turbulence of the second-order with smaller eddies of turbulence. These, in turn, produce turbulence of the third-order. This process continues until the final eddies are so small that they cannot become turbulent. What is left of the kinetic energy of these smallest eddies is transformed into heat as a result of viscosity. This suggests that a large range of scales is created in turbulence, and that this range is larger if we start out with a larger Reynolds number.

This simple notion has been formalized further by *L.F. Richardson* (1920) and, particularly, *A.N. Kolmogorov* (1941). In describing their work, it is

customary to speak loosely of scales of turbulence, which, while being another word for sizes of turbulent eddies, conveys a far less specific picture than balls of fluid moving about in a cohesive manner. For instance, in a Fourier representation of the turbulent velocity, the scale size would be the wavelength of a given mode. The Kolmogorov picture is that the turbulent energy is introduced at the largest scale, say L, which then cascades down to smaller and smaller scales without dissipation until a certain smallest scale is reached, where the velocity gradients are so large that dissipation is large enough to damp out the generation of even smaller scales. The amount of energy transformed into heat per unit volume per unit time, denoted by ϵ, is made up of the mean values of the squares and products of the partial derivatives of u', v', and w' with respect to x, y, and z. One can use ϵ and ν to define the characteristic length and velocity scales of these smallest scales as $l_k = (\nu^3/\epsilon)^{1/4}$ and $v_k = (\nu\epsilon)^{1/2}$. These are known as Kolmogorov length and velocity scales, respectively. It is easy to verify that the Reynolds number based on these scales is exactly unity, consistent with the idea that their order of magnitude corresponds to the smallest dynamical scale in turbulence.

The energy of the intermediate scales between L and η, which form a hierarchy, is given entirely by the consideration that their function is simply to transmit energy to the next smallest scales. Their amplitudes adjust themselves to the requirement that the rate of energy transmission be independent of the scale. Since the time scales associated with smaller length scales is shorter, the energy accordingly diminishes with decreasing scale size in a self-similar manner. Kolmogorov also postulated that the scales will become increasingly isotropic (i.e., direction-independent) as their size becomes smaller.

Following the discussion above, the standard approach is that there are only two length scales of intrinsic interest in turbulence, namely L and l_k. This is not expected to be true near the boundary or if there are multiple mechanisms for the generation of turbulence. Even when it might be true, one can define other length scales. The most popular one is the so-called Taylor microscale λ:

$$\overline{\left(\frac{\partial u'}{\partial x}\right)^2} = \frac{\overline{(u'^2)}}{\lambda^2}\ \text{const.} \tag{7.4}$$

In the case of isotropic turbulence (described in Section 7.4.4), *G.I. Taylor* showed that ϵ is given by the simple expression $\epsilon = 7.5\mu\overline{(\partial u'/\partial y)^2}$. For other forms of turbulence (wall turbulence, free shear flow turbulence), it is not clear that the dissipation can be related to the gradient of a single velocity gradient through a universal numerical coefficient, but the proportionality is still quite frequently applied. If, for brevity, we write u' instead of $\sqrt{\overline{(u')^2}}$, we may put $\epsilon = \text{const}\cdot\mu(u'/\lambda)^2$. Since $u' = l|\partial\overline{u}/\partial y|$, we can put u'/l as an approximation for $|\partial\overline{u}/\partial y|$ and replace $|\tau|$ by $\rho u'^2$ in the equation $\epsilon = \tau'(\partial\overline{u}/\partial y)$. We thus have

$$\mu(u'/\lambda)^2 \cdot \text{const} = \rho u'^3/l,$$

and so

$$\lambda = \text{const}\cdot\sqrt{(\nu l/u')}.$$

If $\text{Re}l = u'l/\nu$ is introduced as the Reynolds number for the motion of an eddy, we have $\lambda \approx l/\sqrt{\text{Re}_l}$.

7.4 Classes of Turbulent Flows

The *mixing length* l in turbulent motion in general varies from place to place. As yet, no general theory is available regarding its magnitude, although in a number of particular cases it has been found possible to make assumptions leading to results in good agreement with experiment. In many cases it is permissible to neglect the actual shearing stresses arising from the viscosity in comparison with the apparent shearing stresses (see remarks above on turbulent transport and mixing). In other instances, the more far-reaching assumption is made that the effect of viscosity on the magnitude of l is negligible. In these cases, therefore, we have to deal with the turbulence of an ideal fluid with zero viscosity. If the Reynolds number is sufficiently large, this point of view appears to be justified.

We shall first discuss two cases in more detail, the so-called free turbulence and the turbulence that arises along a smooth boundary (Sections 7.4.1 and 7.4.2). The effect of viscosity in the latter case, the flow along a rough boundary and the flow past a plate are discussed in Section 7.4.2. Section 7.4.3 deals with stratified fluid and the flow in curved flows, Section 7.4.4 with turbulence in wind tunnels (including some mention of isotropic turbulence), and finally, Section 7.4.5 deals with two-dimensional turbulence.

7.4.1 Free Turbulence

In cases such as the mixing of a free jet having a sufficiently high value of Reynolds number with the fluid surrounding it at rest, it seems reasonable to take the mixing length for every cross-section as being proportional to the width of the jet there ($l = \alpha b$). By b we may, for example, mean half the base of a parabolic or paraboloidal distribution of velocity, in which the maximum velocity and quantity of fluid moving coincide with those of the actual flow considered. Some such assumption is necessary, since the actual flow passes, in an average sense, smoothly into the external fluid without any perceptible boundary. Making an assumption of this kind, we get values for α of approximately 0.125.

Observation shows that free round jets in a sufficiently large space full of fluid at rest spread out in such a way that except in the immediate neighborhood of the outflow, the width of the jet is proportional to the distance

from the point of outflow, while the velocity is inversely proportional to that distance. Throughout the jet the pressure is nearly the same as in the surrounding fluid.

In discussions of an ordinary liquid spray, the assumption is sometimes made that there is a rise of pressure in the air jet as the velocity decreases, by Bernoulli's theorem, and that the pressure at the point of outflow is therefore reduced, thus causing fluid to be sucked up. This is incorrect: Bernoulli's theorem is true only when frictional stresses are absent, which is certainly not the case here. On the contrary, the suction is due to the flow around the edge of the tube that projects into the jet at right angles. In the spreading jet the pressure is practically the same as in the surrounding air at rest.

The decrease in velocity with increase of distance from the point of outflow is therefore due to the frictional stresses alone. Further, the decrease in velocity does not take place in such a way that the same quantity of fluid flows across all cross-sections. That this cannot be the case is clear because, during the advance of the flow, fresh masses of fluid at rest are carried along with it. This is called entrainment of the outer fluid into the jet. On the other hand, the momentum of the jet, $I = \rho \iint u^2 \, da$, is constant on account of the constant pressure. We have $I = \rho u_1^2 \pi b^2 \cdot \text{const}$, where u_1 is the maximum velocity in the cross-section. It follows from the fact that I is constant that u_1 is proportional to $1/b$, i.e., to $1/x$. The flow is that shown in Figure 7.5 and sketched in Figure 4.63.

Another important case is that of the spread of the edge of a jet (Figure 7.6). Here $u_1 = \text{const}$. If we put $l = \alpha b$, we have, as before, $\overline{\tau'} \propto \alpha^2 \rho u_1^2$; i.e., $\overline{\tau'}$ is also constant. The loss of momentum of the part of the flow coming from the pipe is proportional to $\rho u_1^2 b$, and the corresponding resistance is proportional to $\overline{\tau} \cdot x$, so that $b \propto \alpha^2 x$, as in the previous example. (The loss of momentum and the resistance are calculated for a cross-section of unit depth in the direction perpendicular to the plane of the paper.) The fluid sucked in from the surrounding region at rest shows an equal gain of

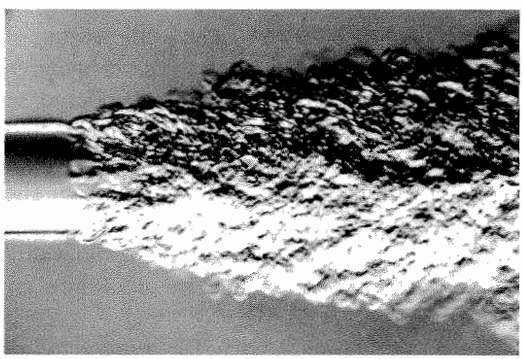

Fig. 7.5. Free jet, *H. Oertel Sr., H. Oertel Jr.* (1989)

momentum. The slope of the boundary between the undisturbed portion of the jet and the turbulent zone is of practical importance. It may be taken as $1:1$.

Yet another case is that of the wake in the rear of a moving body (Figures 4.96 and 4.97). These and other canonical flows have been studied in detail, and a summary can be found in books such as *J.O. Hinze* (1975).

An important development to which we should draw attention is that the instantaneous boundary between the turbulent and nonturbulent parts of free shear flows is quite well defined and relatively sharp at high Reynolds numbers. This is also true of wall-bounded flows on the side exposed to the free stream. Such boundaries, or interfaces, also exist for admixtures. In a given flow, the interfaces for turbulence itself and those for admixtures of

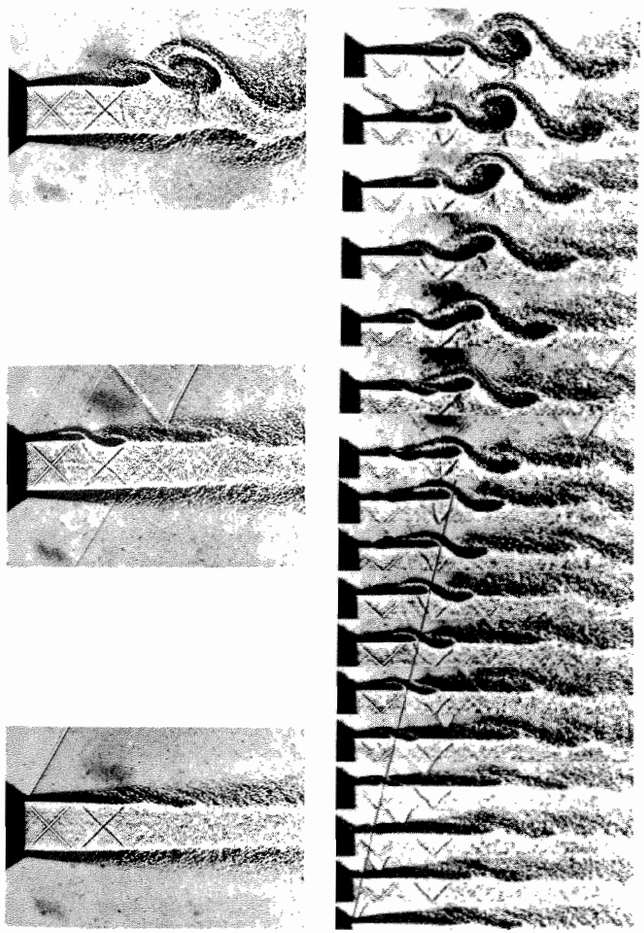

Fig. 7.6. Jet perturbation, *H. Oertel Sr., H. Oertel Jr.* (1989)

various kinds do not necessarily match, either on average or instantaneously. But all these interfaces have convolutions on many scales, from the largest possible to the smallest allowed by viscous or diffusive effects. The stochastic geometry of these boundaries in a range of scales can be described in terms of fractals (see, for example, *K.R. Sreenivasan* (1991)).

7.4.2 Flow Along a Boundary

In cases of flow along boundaries, the *mixing length* must tend to zero as the boundaries are approached. This is clear from the definition of the mixing length. It follows from this that $\partial\overline{u}/\partial y$ becomes very small in the interior of the flow but reaches large values in the neighborhood of the boundaries. Figure 4.54 shows the differences between the distributions of velocity for turbulent flow and laminar flow in a tube.

Following Section 4.2.4, we might regard that the layer of fluid next to the boundary adheres to it even in the case of turbulent flow, and in the immediate neighborhood of the boundary a thin sublayer is formed with $\partial\overline{u}/\partial y = \tau_{\text{wall}}/\mu$, provided that the boundary is smooth. It should be stressed that the viscous sublayer is highly disturbed and is far from being laminar, as it once was thought to be. For large values of the Reynolds number, the value of τ_{wall} is quite considerable, owing to the vigorous mixing in the interior of the fluid, so that the rate of increase $\partial\overline{u}/\partial y$ is extremely rapid, and the viscous sublayer is accordingly very thin. For a superficial observation, it thus seems as if in turbulent motion the velocity has a finite value even at the boundary itself.

From the theoretical point of view, a general idea of the state of affairs may be obtained simply if we assume that the shearing stress is constant throughout the region outside the viscous layer. In actual cases of flow, τ decreases continuously as the distance from the boundary increases beyond a point. (For the pipe, τ becomes zero on the axis.) Nevertheless, the formulas obtained by putting $\tau = \text{const} = \tau_{\text{wall}}$ give very useful approximations even in this case, since the greater part of the velocity change occurs very close to the boundary. For pipes, the formulas below hold nearly to the axis, since here l lags behind κy as the distance from the wall increases. If this is positive, $\partial\overline{u}/\partial y$ is also positive. The total shearing stress ($\tau = \overline{\tau} + \tau'$, the mean value of the viscous stress plus the apparent shearing stress due to turbulence) is then given by

$$\tau = \mu\frac{\partial\overline{u}}{\partial y} + \rho l^2\left(\frac{\partial\overline{u}}{\partial y}\right)^2. \tag{7.5}$$

The first term is important only for very small distances from the boundary. If the Reynolds number is fairly large, the second term is so much greater than the first (except close to the boundary) that the first may be neglected in comparison with it. Taking the square root of the resulting simplified form of equation (7.5), we have

$$\sqrt{\frac{\tau}{\rho}} = l\frac{\partial\overline{u}}{\partial y}. \tag{7.6}$$

From the right-hand side we readily see that $\sqrt{(\tau/\rho)}$ has the dimensions of a velocity. For simplicity, we introduce the symbol u_τ and call it the friction velocity. It is of the same order of magnitude as the velocities u', v' due to turbulence (or, more accurately, $u_\tau = \sqrt{\overline{(u'v')}}$). With the assumption we have made here, however, u_τ may be regarded as constant.

We shall now suppose that $y = 0$ represents a smooth wall, and, for simplicity, regard it as extending to an infinite distance in both horizontal directions. We shall assume that another wall is at an infinite distance away from the first wall. Then $\overline{u}$ depends on y only. In what follows, therefore, we shall write $d\overline{u}/dy$ for $\partial\overline{u}/\partial y$, and since we shall no longer be concerned with fluctuations, we shall also drop the averaging.

We have now to find a reasonable law for the mixing length l, i.e., one that gives the correct dimensions. If we make the further assumption (suggested by observation) that l is unaffected by fluid viscosity, the only length we have at our disposal is the distance from the wall y. The only dimensionally correct formula for l is then

$$l = \kappa y. \tag{7.7}$$

The numerical factor κ is essentially a universal constant of this problem in turbulent flow. It is known as the Kármán constant, due to *Th. von Kármán*. From equation (7.6) we then have

$$u_\tau = \kappa y\frac{du}{dy}. \tag{7.8}$$

Since u_τ is constant, this can be immediately solved, giving

$$u = u_\tau\left(\frac{1}{\kappa}\ln y + C\right) \quad , \tag{7.9}$$

For large values of the Reynolds number this expression is in reasonable agreement with observation, with 0.41 as the accepted value of the Kármán constant. (It is true that for $y = 0$ the formula gives the value $-\infty$ instead of the value 0, but we know already that our simplified calculation will not apply at or near $y = 0$; instead, we should have to use the more accurate equation (7.5) and set up a modified formula for l involving the second length ν/u_τ. We shall discuss the role of this second length scale later.)

We can also obtain an expression for C, the constant of integration in equation (7.9), from the fact that the viscosity becomes important in the immediate neighborhood of the wall. The expression in parentheses in equation (7.9) must be a pure number and must not depend on the units employed. This is achieved if we subtract from $\ln y$ the logarithm of the length ν/u_τ mentioned above, i.e., if we put

$$C = C_1 - \frac{1}{\kappa}\ln\frac{\nu}{u_\tau}. \tag{7.10}$$

Then C_1 is a second universal number, and we have

$$u = u_\tau\Big(\frac{1}{\kappa}\ln\frac{yu_\tau}{\nu} + C_1\Big). \tag{7.11}$$

Since the greatest velocity differences occur in the immediate neighborhood of the wall, equation (7.11) may also be used as a good approximation in cases in which the shearing stress τ depends on y. We have merely to set $u_\tau = \sqrt{(\tau_{\text{wall}}/\rho)}$, and obtain values of the velocity that are found to lie very close to the observed values. For these cases that deviate from the theory, e.g., for flow in pipes, the observed values of u/u_τ can be plotted against $\log_{10}\frac{yu_\tau}{\nu}$. The curve obtained is almost a straight line. If equation (7.11) is used in this way as an approximation to the distribution of velocity in smooth-walled straight pipes, Nikuradse's experiments (*J. Nikuradse* 1932) give $\kappa = 0.40$ and $C_1 = 5.5$. Passing from natural logarithms to ordinary logarithms ($\ln x = 2.3026\log_{10} x$), we obtain

$$u = u_\tau\Big(5.6\log_{10}\frac{yu_\tau}{\nu} + 5.5\Big). \tag{7.12}$$

M.V. Zagarola and *A.J. Smits* (1998) have recently extended the range of pressure drop measurements in a pipe up to about 36 million in the Reynolds number based on the pipe diameter, thus extending Nikuradse's range by a factor of about 10. They confirm the existence of a logarithmic region (though the Kármán constant in these measurements is a few percent lower).

It should be mentioned that there is a different scheme of describing the velocity distribution in pipe flows (and, in general, in wall-bounded flows). This scheme, in its modern form, is due primarily to *G.I. Barenblatt* (1993). It proposes that (7.8) is not strictly valid because the influence of the second length scale, namely ν/u_τ, never strictly disappears but remains in tact, though perhaps only weakly. Loosely speaking, this expectation is in keeping with the spirit of the behavior of condensed matter near the critical point. Instead of equation (7.8), one then has

$$\frac{\mathrm{d}u}{\mathrm{d}y} = \frac{1}{\kappa}\frac{u_\tau}{y}\Big(\frac{yu_\tau}{\nu}\Big)^\beta, \tag{7.13}$$

where β is an undetermined constant. Integrating the equation, one can see that a power law emerges for the velocity distribution. *Barenblatt* and his collaborators have examined the data of *Nikuradse*, and also those of *Zagarola and Smits* in the lower range of Reynolds number, and concluded that the power law provides a better fit to the velocity distribution than the logarithmic law. They have determined the constants in the power-law velocity distribution by empirical fit to the data.

This description is not merely one of which of the two forms fits the data better, but is one of principle: Even at high Reynolds numbers, and not too close to the wall, does the influence of the second length scale ν/u_τ disappear altogether, or remain weakly present? A firm answer to this question will have a basic consequence to our thinking on how one quantity scales with another

in wall-bounded flows. At the moment, there is still considerable debate as to whether the logarithmic or the power law is a proper description in the region not too close to the wall.

7.4.3 Rotating and Stratified Flows, Flows with Curvature Effects

So far, we have assumed that Earth's rotation and density stratification that are evident in most natural flows are of no consequence in turbulence. This is true to a large measure in laboratory flows, though these effects can be important even on that scale. One need only consider the bathtub vortex and its direction of rotation of the fluid as it nears the drain. Large-scale flows such as hurricanes are clearly affected by both Earth's rotation and density stratification.

The main effect of rotation is to introduce centrifugal and Coriolis forces. The centrifugal force always acts perpendicular to the axis of rotation, and is similar in structure to the pressure gradient, with which it is often considered together. In the case of the flow past curved objects, turbulence is diminished or increased as a result of the centrifugal forces, according to whether the velocity increases or decreases from the center of curvature outwards. Here the variation in magnitude of the centrifugal forces plays the same role as that played by variation of the force of gravity in the flow of layers differing in density.

M. Couette (1890) investigated a fluid in the space between two cylinders, the outer (radius r_1) rotating and the inner (radius r_2) at rest. If the gap $d = r_2 - r_1$ between the cylinders is small compared with r_1 and r_2, there is a critical peripheral velocity v such that the Reynolds number $u_\phi d/\nu$ is equal to 1900. If the distance between the cylinders is greater, then the stabilizing effect of the centrifugal forces mentioned above comes into play, and the critical value of Reynolds number rises sharply. On the other hand, if the inner cylinder rotates and the outer one is at rest, even the streamline motion is unstable, regular eddies being formed with their axes parallel to the direction in which the periphery is moving and with alternate right-handed and left-handed directions of rotation (see Figures 7.7 and 8.33). A condition for the occurrence of this instability was obtained by *G.I. Taylor* (1923) and confirmed by experiment. It may be expressed as follows:

$$\frac{u_\phi d}{\nu} > 41.3\sqrt{\frac{r}{d}}, \tag{7.14}$$

where r is the mean of the two radii.

The stability or instability just mentioned is noticeable in turbulent boundary layers at surfaces of comparatively slight curvature. The turbulent mixing is hampered at convex surfaces and strengthened at concave surfaces. Eddies similar to those of Taylor, described above, may even occur in laminar flow past concave surfaces. According to *H. Görtler* (1941), if δ is the

thickness of the boundary layer, $U\delta/\nu = 16\sqrt{(r/\delta)}$ may be regarded as the limit of stability (see Section 8.3.2).

Examples of the turbulent velocity profile between a rotating cylinder and a nonrotating cylinder are given in Figure 7.8, based on experiments by *F. Wendt* (1933). The exchange of momentum is small if the outer cylinder rotates, but large if the inner cylinder rotates.

The Coriolis force, which acts perpendicular to the axis of rotation and is perpendicular to the relative velocity, may be explained as follows. If a fluid mass moves from Earth's equator to the north, it crosses latitudes with decreasing radius. To preserve its angular momentum, the fluid parcel has to spin faster and thus move to the right. A fluid parcel moving toward the equator will have to slow down and move, relative to Earth, to the left. The movements in the Southern Hemisphere are just the opposite. The Coriolis force, which thus depends on the latitude, is proportional in magnitude to the sine of the latitude, and is a source of additional vorticity, and turbulence, in rotating systems (see Chapter 12).

The precise circumstances in which the Coriolis force is important depend on the relative magnitude of other forces. The ratio of inertial to Coriolis forces is called the Rossby number. A second parameter, called the Ekman number, is the ratio of frictional forces to the Coriolis force. In most geophysical flows (which include atmospheric and oceanic motions), the inertial force is by far stronger than the frictional force, so it is often the Rossby number that is important. In the boundary layers, of course, the Ekman number is also of consequence.

An additional effect is due to density stratification. In a flow that is predominantly horizontal, if the density of the medium diminishes rapidly

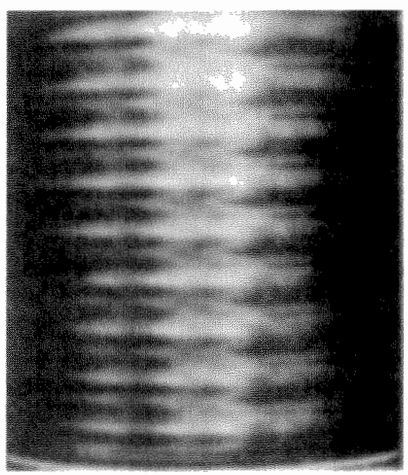

Fig. 7.7. Taylor instability

upward (as, for example, in a mass of air with the temperature increasing upward, or where there is a layer of fresh water superimposed on salt water), the process of turbulent mixing must cause heavier layers to be moved above the lighter, and lighter layers to be pushed down below the heavier. That is, part of the work available for the maintenance of turbulence (derived from the main flow) is used up against gravity. This may cause the turbulent motion to be diminished and possibly die out altogether. This is the explanation of the cessation of turbulence and dying down of the wind at night in the lower layers of the atmosphere (the wind still continuing unabated at a higher level). Conversely, turbulence is increased by irradiation from the ground, which causes a reversal of the stratification, resulting in dense layers higher than less dense ones. This is what happens, for example, in so-called Rayleigh–Bénard convection, in which a fluid layer contained between two horizontal plates is heated at the lower plate and cooled at the top plate.

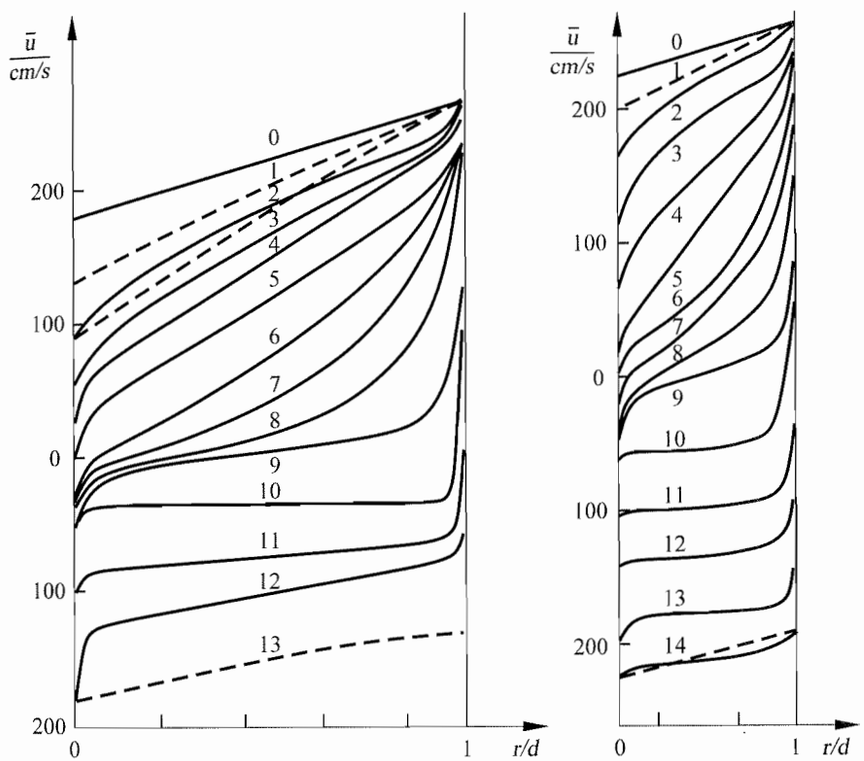

Fig. 7.8. Turbulent velocity profiles in the cylindrical gap of a rotating and a fixed cylinder, *F. Wendt* (1933)

7.4.4 Turbulence in Tunnels

Much attention has been devoted to turbulence in wind tunnels. Here turbulence is undesirable, since one object of experiments in wind tunnels is to simulate the state of affairs when a body is moving at a uniform speed through air at rest. Turbulence, however, cannot be entirely avoided. Residual turbulence remains even after the air has passed through a honeycomb and screens at the entrance section of the tunnel (see Figure 7.9). This particularly affects the occurrence of turbulence in the boundary layers on bodies under investigation, and hence also the separation of the flow from the bodies. Separation changes the character of the flow near the wall and affects transport properties immensely. Needless to say, controlling the wind-tunnel turbulence is especially important in studies of laminar-to-turbulent transition in boundary layers and other flows.

The earliest way of measuring turbulence in a wind tunnel was by the fall in the drag of a sphere due to the onset of turbulence in the boundary layers. Later, *G.B. Schubauer, H.K. Skramstad* (1947), and *H.L. Dryden* (1948) worked out methods using hot-wire anemometers, by which numerical values for the small fluctuations of velocity could be obtained more or less reliably. It was found that wind-tunnel turbulence (or, more generally, any turbulence arising from flow through a grid of bars) has simple properties at sufficient downstream distances from it. It is found to be nearly *homogeneous and isotropic*; that is, the fluctuations of velocity are of the same magnitude across the wind tunnel cross-section, and their magnitude is the same in all directions as well. Homogeneous and isotropic turbulence is therefore the simplest form of turbulence, and can be dealt with up to a point by statistical theory and by experiments suggested by theoretical work. Special reference should be made to the papers by *G.I. Taylor* (1935, 1936), who introduced the concept, and *Th. von Kármán* (1948), who was responsible for deriving an important equation for statistical quantities from the Navier–Stokes equations.

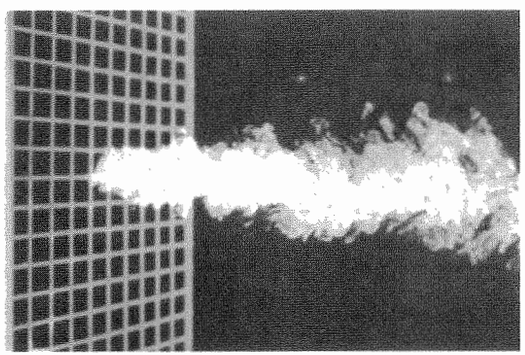

Fig. 7.9. Turbulent flow behind a wind-tunnel honeycomb, *M. Lesieur* (1997), picture by *J.L. Balint et al.*

The simplest statistical quantity is the mean energy of fluctuation

$$E = \frac{1}{2}\rho\left(\overline{(u'^2)} + \overline{(v'^2)} + \overline{(w'^2)}\right). \tag{7.15}$$

From a series of measurements made for a grid of mesh-width m through which fluid moves with mean velocity U, it is now known that q behaves as a power of the distance from the grid. Equivalently, in situations where the turbulence is generated by sweeping a grid of bars at velocity U through a fluid medium at rest, the decay of the energy changes as a power law in time. The power-law exponent is roughly -1.25. It is not clear whether this exponent is universal, or depends weakly on a number of features such as m, the diameter of the rod, the geometry of the rod itself, and on whether the grid is passive or has some moving elements to it. The constant of proportionality in the formula is indeed nonuniversal and depends strongly on the details just mentioned.

An idea of the distribution in space of the fluctuations in velocity may be obtained by studying the correlation between the velocities at neighboring points A and B. For isotropic turbulence there are only two nonzero correlations, both functions of the distance $r = \overline{\mathrm{AB}}$. In Figure 7.10, R_1 is the correlation between the components of velocity at A and at B parallel to the line AB separating the two points, and R_2 the correlation between two parallel components of velocity at A and at B at right angles to the line AB. Because of continuity, it can easily be proved, as was done by *Th. von Kármán*, that R_1 and R_2 are connected by the relation

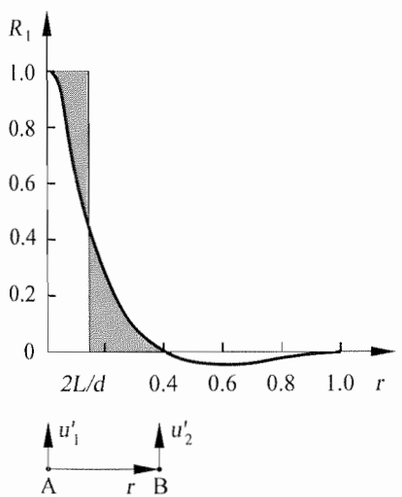

Fig. 7.10. Correlation of velocity fluctuations

$$r\frac{\mathrm{d}R_1}{\mathrm{d}r} = 2(R_2 - R_1). \tag{7.16}$$

From the graph of R_1 the characteristic length of turbulence can be derived: $\int_0^\infty R_1(r)\mathrm{d}r = L$. It is closely related to the mixing length l. The value of L in Figure 7.10 is a measure of the large eddies in the turbulence motion, in which the energy of turbulence is controlled by the manner in which turbulence is produced. According to *G.I. Taylor* (1936), the statistical mean value of the dissipation is proportional to

$$\mu q^2 \left(\frac{\mathrm{d}^2 R}{\mathrm{d}r^2}\right)_{r=0},$$

where

$$\left(\frac{\mathrm{d}^2 R}{\mathrm{d}r^2}\right)_{r=0} = \frac{1}{\lambda^2}. \tag{7.17}$$

The Reynolds number based on λ, the Taylor microscale introduced earlier, and the root-mean-square fluctuation velocity u', are often used to compare properties among different flows for which the characteristic large scale depends on the geometry, and is thus not a useful scale of comparison. It should be remembered that λ does not represent the smallest scales of turbulence. That indication is provided by the Kolmogorov scale l_k, already mentioned in Section 7.2.3.

Isotropic Turbulence

As the name suggests, isotropic turbulence (see Figure 1.4) has no directional preference and is a mathematical construct: In fact, turbulence can be generated only in the presence of local shear or near boundaries, and the process of generation of turbulence tends to maintain a preferred direction. However, the turbulence that is found far enough away from the boundary where the mean velocity gradients are small is often approximately isotropic. Isotropic behavior can often be a good first approximation when deviations from it are not large. Further, smaller scales of turbulence tend to be statistically isotropic (though individual structures do show deviations from isotropy). For all these reasons, isotropic turbulence is of some interest. In any case, this is the form of turbulence most accessible to theoretical development, and has consequently assumed an importance in its own right. Isotropic turbulence is also homogeneous, though the mention of the latter is often omitted for brevity.

The main technical problems in isotropic turbulence are the nonlinear transfer of energy from one scale to another, and its dissipation to heat. On average, the energy transfer occurs from large scales to small scales, though instantaneously, there is some two-way transfer. The average transfer is assumed to proceed from one scale to a neighboring smaller scale in the form of an energy cascade. When the scales involved are large, that is, their characteristic Reynolds numbers, based on their own size, are sufficiently high, it is assumed that the scales merely transmit energy to the next smaller ones without dissipating any part of the energy. When the energy reaches the smallest scales, it is presumed to be dissipated there. This is the so-called Richardson cascade, due to *L.F. Richardson* (1920). If the picture holds for any type of turbulence at all, isotropic turbulence is the most likely candidate.

One consequence of the energy cascade is that when the scales that contain most of the energy (of order L) and the scales that dissipate most of the energy (of order l_k) are significantly different, the energy dissipation rate is the same as the rate at which energy is being pumped into turbulence at large scales. This equality has been verified both experimentally in grid turbulence and by solving the equations of motion on a high-speed computer, as long as the Reynolds number of turbulence is sufficiently high for the said scale separation to exist. Thus arises the notion that the energy dissipation rate in high-Reynolds-number turbulence is independent of fluid viscosity. This seemingly anomalous behavior is of great consequence, and shows that the limit of high Reynolds number (or vanishing viscosity) is not the same as the case of zero viscosity. It may be recalled that this feature is common to all singular perturbation problems including boundary layers.

The most significant work in isotropic turbulence is due to *A.N. Kolmogorov* (1941), which follows naturally from the Richardson cascade. Though Kolmogorov's work was motivated by isotropic turbulence, its description is better postponed to a later section that considers small scales of turbulence. The reason is the widely held perception that small scales of turbulence are statistically isotropic, independent of the nature of large scales, or, equivalently, of the manner of producing turbulence. But one result should be mentioned here. In the so-called inertial range of scales, which is smaller than the energy-containing scales L and larger than the dissipating scales l_k, the energy transfer process adjusts itself so that the spectral distribution of energy is given in the form

$$E(k) = C_k \epsilon^{2/3} k^{-5/3}, \tag{7.18}$$

where C_k is the so-called Kolmogorov constant and ϵ is the rate of energy dissipation. The integral of $E(k)$ over all wave numbers k gives the total turbulent kinetic energy. Here, the wave number k takes the role of distinguishing different scales of turbulence: Small values of k correspond to large scales, and large k represent small scales. The constant C_k cannot be deduced theoretically but is known from experiment to be a constant of about 0.5 at high Reynolds numbers.

In the past, isotropic turbulence has been studied in wind tunnels behind a grid of bars, or by pulling a grid of bars through a stationary mass of fluid. Recently, as computer power has increased, the Navier–Stokes equations (see Section 5.2) have been solved numerically, starting with an initial realization of a prescribed random field. In due course, the computer solutions attain properties that are essentially independent of the initial conditions and replicate those of measured turbulence. Such simulations have provided a very

powerful tool for understanding turbulence in general, and isotropic turbulence in particular. An interesting result to emerge is that the structure at small scales is in the form of vortex tubes that are long compared to their diameter. The vortex tubes form mosaics of several different scales. It is not yet clear whether this observation is of some fundamental consequence to the theory of turbulence.

7.4.5 Two-Dimensional Turbulence

As a rule, the components of turbulent fluctuating velocities in all three directions are of the same order of magnitude except close to solid surfaces, or when certain types of body forces act on the flow. This is true even in flows that are two-dimensional on average (such as boundary layers on extended flat plates, or wakes behind long cylinders, which do not have any average variations along the span). There are circumstances, however, in which turbulence is close to being two-dimensional (i.e., fluctuations are largely planar). Examples are atmospheric and oceanic flows (see Chapter 12), which often have a very large spatial extent in two directions and a relatively short extent in the direction of their depth. Such flows occur in a stratified, often rotating, environment and are central to understanding and predicting weather, dispersion of particles and chemicals in the atmosphere and oceans, and other natural phenomena. Another example of two-dimensional turbulence is the turbulent flow in a soap, which is shown in Figure 7.11.

While these examples are not purely two-dimensional, there is promising evidence that the strictly two-dimensional mathematical approximation will allow us to make some headway. On the experimental front, there has been some success in generating in the laboratory close approximations to two-dimensional flows that compare well to both natural flows and the mathematical ideal. Two-dimensional turbulence is also studied with the expectation that it could provide insight into the three-dimensional problem. For instance, the two problems have in common fundamental properties such as energy transfer between scales, dissipation mechanisms, and structure formation and evolution.

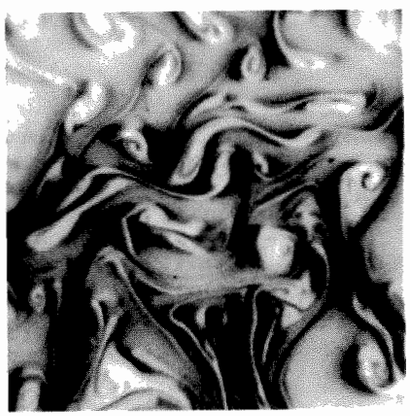

Fig. 7.11. Turbulent flow in a soap, *P. Vorobieff, R.E. Ecke* (2003)

Major Theoretical Results

The relative simplicity of the two-dimensional Navier–Stokes equation allows several fundamental properties to be derived. The first result can be derived in a straightforward manner by taking the curl of the Navier–Stokes equation for an incompressible fluid, and taking the inviscid (Euler) limit. We obtain the Helmholtz theorem

$$\frac{\partial \omega}{\partial t} + \boldsymbol{u}\nabla\omega = 0, \tag{7.19}$$

where the vorticity $\omega = \nabla\times\boldsymbol{u}$ is always along the axis normal to the plane. Here arises a fundamental difference to the situation in three dimensions: The Helmholtz equation means that vorticity of a fluid parcel is conserved through the lifetime of turbulence. In contrast, three-dimensional turbulence permits an additional vortex-stretching term ($\omega\nabla\boldsymbol{u}$), which is nonzero due to the presence of the additional degree of freedom in the third dimension. Furthermore, the restriction to the plane results in the following equations for energy $E = \frac{1}{2}\langle \boldsymbol{u}^2\rangle$ and enstrophy $\Omega = \langle\omega^2\rangle$ in two-dimensional homogeneous turbulence

$$\begin{aligned} \frac{dE}{dt} &= -\nu\Omega, \\ \frac{d\Omega}{dt} &= -\nu\langle(\nabla\omega)^2\rangle. \end{aligned} \tag{7.20}$$

For three-dimensional turbulence, the zero-viscosity limit is known to lead to an increase of enstrophy, because viscous diffusion of vorticity decreases, and stretching of vortex lines is less restrained. Thus, as already mentioned, the rate of energy dissipation for three-dimensional turbulence remains finite even in the inviscid limit. In two dimensions, however, the enstrophy changes only due to viscous effects, and thus can only decrease. This leads to zero rate of energy dissipation in the inviscid limit. *G.K. Batchelor* (1948) provided arguments that the rate of dissipation of enstrophy is nonzero in the inviscid limit in the two-dimensional case; this is the so-called enstrophy dissipation anomaly.

The final picture, then, is that two-dimensional systems do not dissipate energy in small scales. The energy is transported to larger scales and eventually gets dissipated by friction at the boundaries of a finite system. On the other hand, enstrophy is allowed to cascade down the scales to be dissipated in the small scales. Therefore, there appears to be some (limited) value to casting the two-dimensional enstrophy (vorticity) as analogous to three-dimensional energy (velocity). This was the approach of *R.H. Kraichnan* (1967).

The Energy and Enstrophy Cascades

R.H. Kraichnan (1967) recognized that the enstrophy and the energy cascades can exist simultaneously in two dimensions. From the study of the conservation equations and triadic wave number interactions, it can be shown that energy is transferred, on average, toward the small wave numbers (large scales), while the enstrophy is transferred toward the large wave numbers (small scales). The prediction for the energy spectrum in the inverse cascade is a scaling law $E(k) \propto k^{-5/3}$, which has been verified in numerical simulations and experiments. This behavior of the energy in two-dimensional turbulence is in marked contrast to the three-dimensional case. The inverse energy cascade implies a mechanism by which large eddies are created from small eddies instead of the other way around. The phenomenological picture is that the initial vortices, formed by the forcing, get conjoined to other vortices to form larger ones during their lifetime, i.e., in the time it takes for friction at the boundary to damp them out by depleting all their energy. The three-dimensional Richardson cascade of the breakup of eddies is replaced by an aggregation process among vortices in two dimensions. The Kraichnan conjecture for a (stationary) inverse cascade seems to hold only if there is a sink for energy at large scales. While the fluid itself has no such property, the boundary conditions in both simulations and experiments provide the artificial sink for energy, for example, the friction at the walls. This allows for observation of a sustained (stationary) inverse energy cascade. One example of a cascading decay of a sinking vortex ring is shown in Figure 7.12.

The enstrophy Ω, as already mentioned, is dissipated in the small scales in the inviscid limit. In a forced two-dimensional system the enstrophy cascades from the energy injection scale down to the small scales. The enstrophy spectrum in the inertial range, according to Kraichnan's theory, has the behavior

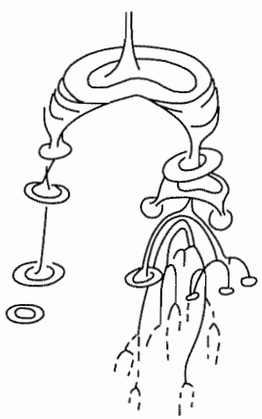

Fig. 7.12. Cascading decay of a vortex ring, *H.J. Lugt* (1983)

$\Omega(a) \propto k^{-1}$. It may be recalled that the corresponding energy spectrum in the inertial range was predicted to be $E(k) \propto k^{-3}$. Experimental observations of the decaying energy spectrum have yielded slopes ranging from -3 to -4 over varying times and ranges of initial conditions. A full description of these aspects are summarized by *P. Tabeling* (2002).

Structures

Both forced and decaying two-dimensional turbulence have a well-documented tendency to form coherent structures. There is as yet no theoretical understanding of this phenomenon, and the definition of a coherent structure remains vague. The remarkable feature of the two-dimensional coherent structures observed in both numerical and experimental work is their long lifetimes. Much energy has been put into identifying coherence in vortical structures, determining their stability properties, and analyzing the dynamics of vortex interactions including merging. Examples of coherent structures in turbulent flames are discussed in detail in Chapter 11. Figure 7.13 shows a laser-induced fluorescence sheet (LIF) of the OH concentration of a turbulent premixed air–gas flame.

One approach to studying coherent structures in two dimensions is complementary to the great amount of work already present in three dimensions. The goal is to provide a statistical description of freely decaying two-dimensional turbulence. *G.K. Batchelor* (1969) was the first to propose self-similarity in time of the decay process. A dimensional argument then led to

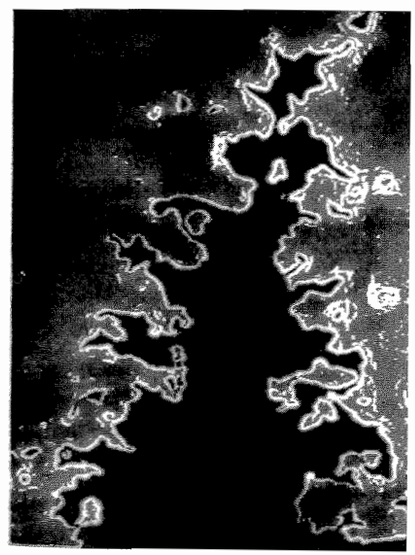

Fig. 7.13. Coherent structures in a turbulent flame (see Section 11.3.8)

the following estimate of the decay rate of the vortex density ρ,

$$\rho \propto E^{-1}t^{-2}, \tag{7.21}$$

where E is the kinetic energy density. The same dimensional analysis shows that both vortex size and intervortex spacing grow at a rate linear in time t. This was the initial attempt at a statistical description. It was soon discovered in numerical simulations that although power laws seem to hold, the exponents deviated from Batchelor's prediction. The vortex density decayed more slowly, as did the growth of their size and spacing. These numerical observations have more recently been supported by experimental data. It has also been proposed that another invariant must be present in the system in addition to E. This invariant is the global maximum vorticity of the system. While the physical justification for this quantity as an invariant of a decaying system is not rigorous, it seems to derive reasonable numerical support. On recalculation of the scaling exponents, good agreement with empirical evidence is achieved, supporting this framework, known as the *universal decay theory*.

7.5 New Developments in Turbulence

The past few decades have seen an increased interest in the statistical descriptions of turbulence, and the desire to incorporate the observed structure in such descriptions. While turbulence involves the creation and interaction of structures and patterns of different length scales, its vast spatial and temporal complexity necessitates a stochastic description. It is hoped that a probabilistic description will yield a simplified picture of its universal properties. The length scales within which universality may be applicable are much smaller than the large scale L, which characterizes the size of the system, or of the manner in which turbulence is generated. The focus on the small scales, while offering plenty of promise, tends to gloss over large-scale phenomena such as structure formation and coherence, and sweeping effects on the small structures. Certain properties of the large-scale motion are *also* universal, in the sense that they have an origin in some large-scale instability, but they are nonuniversal in that their shapes, onset, and precise manifestation differ from flow to flow. The two regimes of turbulence, namely the small and large scales, have often been examined independently of each other, based on the assumption that sufficient separation between them offers independence from each other. In reality, of course, this independence is to be regarded only as a convenient model.

We first present a summary of the experimental methods in use, and then discuss some of the recent work.

Experimental Methods

The measurement of small-scale, rapidly fluctuating quantities such as velocity and velocity derivatives is still most successfully done using thermal anemometry and hotwire probes (see, e.g., *H.H. Brunn* (1995) for a survey of the methods). Data from such measurements are used to calculate statistics of flows ranging from mean properties to high-order moments such as Reynolds stress and structure functions (which are moments of velocity differences between two neighboring points in space). The limitation of hotwire data is that their spatial information is always obtained by some means of surrogation, for instance the use of Taylor's hypothesis, which assumes that the flow is swept past a probe, without any distortion, at the local speed. Of course, multiple probes can be, and have been, used, but there is a limit beyond which this escalation becomes both cumbersome and invasive. In its simplest form, laser Doppler velocimetry (LDV) again yields single-point measurements. The advantage of LDV is that it is nonintrusive and can be used in hostile environments such as flames. The need for full spatial information has led to the development of particle image velocimetry (PIV). However, the advantage of PIV over hotwire (or LDV) is restricted by the present technology, which places limits on the temporal resolution attainable, and hence on resolution of the fluctuations at high Reynolds numbers. A recent effort to remedy this constraint of classical PIV has been made. High-energy particle detectors were modified to serve as optical imaging devices for tracking particles in a high-Reynolds-number flow (*G.A. Voth et al.* (1998)). Finally, the incentive to create very high Reynolds number flows under controlled laboratory conditions has motivated the use of low-viscosity cryogenic helium as a test fluid (see, e.g., *K.R. Sreenivasan, R.J. Donnelly* (2000)). In this method, very high Reynolds numbers can be achieved in moderately sized apparatus.

Small-Scale Turbulence

To study small-scale turbulence, one needs measures that are independent of the large-scale motion on which small scales are superimposed. A simple such measure is the velocity difference between two points separated by a distance r that is small compared to the large scale L. It is generally assumed that such quantities, for $r \ll L$, behave as in isotropic turbulence. This is the assumption of local isotropy. The rate at which anisotropic effects of the large scale diminish with the reduction in scale is a subject of much study and practical interest, and a survey of the work can be found in *S. Kurien, K.R. Sreenivasan*, (2001).

One exact relation valid at high Reynolds numbers is the so-called Kolmogorov's law, according to which the following relation holds exactly in the inertial range $l_k \ll r \ll L$:

$$\left\langle (u(x+r) - u(x))^3 \right\rangle = -\frac{4}{5}\langle \epsilon \rangle r. \tag{7.22}$$

This law has provided the basis for an enormous volume of work. The classical interpretation of equation (7.22) (e.g., *A.S. Monin, A.M. Yaglom* (1975)) is that the energy flux from large to small scales is unidirectional on average. Other attempts have been made to extract more information from this equation. The equation fixes the extent of the inertial range in experiments and in estimates $\langle\epsilon\rangle$ with less ambiguity than by the local isotropy relation $\langle\epsilon\rangle = 15\nu\left\langle(\partial u/\partial x)^2\right\rangle$.

Extrapolating the implications of Kolmogorov's arguments for higher-order moments of velocity increments, we have

$$\langle(u(x+r)-u(x))^n\rangle = C_n(\langle\epsilon\rangle r)^{n/3}. \tag{7.23}$$

The spectral equivalent of equation (7.23) for the special case with $n = 2$ can be written as

$$\phi(a_1) = C\langle\epsilon\rangle^{2/3}a_1^{-5/3}, \tag{7.24}$$

where $\phi(a_1)$ is the one-dimensional spectrum of the wave number component a_1, and C_k is called the Kolmogorov constant, mentioned already. *H.L. Grant et al.* (1962) verified equation (7.24) for the first time. Subsequent investigators have also found the spectral slope to be close to 5/3. Existing data show that the Kolmogorov constant is approximately constant (0.5 ± 0.05) over a wide range of Reynolds numbers.

In the dissipation range, Kolmogorov's arguments yield the following result for the spectral density:

$$\phi(a_1) = f(K)\langle\epsilon\rangle^{2/3}a_1^{-5/3}, \tag{7.25}$$

where $K = a_1 l_k$ is the wave number normalized by the Kolmogorov length scale $l_k = (\nu^3/\langle\epsilon\rangle)^{1/4}$, and the universal function $f(K)$ is unknown (except that it approaches C for small K). From numerical simulations at low Reynolds numbers, it appears that the spectral density is of the form $K^{a'}\exp(-ga)$, where $a' \approx 3.3$ and $g \approx 7.1$, though it appears to be smaller at higher Reynolds numbers. Experimental data support equation (7.25) to some extent, but the data collapse is not fully satisfactory. A different type of spectral universality in the dissipation region has been proposed on the basis of multifractality of the small scale. For a discussion of this approach, see *U. Frisch* 1995.

The present situation is such that it is not possible to state that (7.23) works exactly, even for second-order statistics. There certainly appear to be departures from equation (7.23) for large enough n. In atmospheric boundary layers, in high-Reynolds-number air and helium flows, the probability density functions of the velocity increments in the inertial range vary continuously with scale separation r. If fitted by stretched exponentials $e^{\Delta u_r^m}$, the stretching exponent m varies smoothly with r, from about 0.5 in the dissipative range to about 2 as r approaches integral-scale separations (i.e., the distribution becomes a Gaussian). If Kolmogorov were right, m would be a constant independent of r. Given the empirical evidence, one is forced to give up the Kolmogorov universality in its broadest sense, though it remains of considerable value in making estimates at most finite Reynolds numbers.

Intermittency in the Inertial and Dissipation Ranges

It is now believed, following *A.M. Obukhov* (1962), that the reason for the failure of Kolmogorov's universality is the strong variability of the energy dissipation rate, a phenomenon known as *intermittency*. Obukhov suggested replacing the (global) mean energy dissipation rate $\langle\epsilon\rangle$ in Kolmogorov's formulas by the local average value ϵ_r defined over a ball of radius r. For $r \ll L$, where L is a characteristic large scale, the variable $\epsilon_r/\langle\epsilon\rangle$ is a fluctuating quantity and, according to *Obukhov's* suggestion, a function of the ratio r/L. In this way, whenever averages are taken over regions containing varying levels of energy dissipation rate, the large scale enters inertial-range statistics explicitly. *A.N. Kolmogorov* (1962) made *Obukhov's* suggestion more explicit by assuming that the dissipation rate is lognormally distributed. He also refined his original hypotheses in an essential way by taking note of *Obukhov's* suggestion. This gave rise to the so-called refined similarity hypothesis. The resulting modification is that one may expect power laws of the form

$$\langle\Delta u_r^n\rangle/u_0^n = C_n'(r/L)^{\zeta_n}, \tag{7.26}$$

where the large-scale velocity u_0 and the factors C_n' are nonuniversal, but the exponents ζ_n, although different from $n/3$, are presumed to be universal. The deviation of the exponents ζ_n from $n/3$ is the hallmark of inertial-range intermittency. Inertial range intermittency is also deduced from the empirical fact that the probability density functions of wave number bands show increasingly flattened tails for increasing midband wave numbers.

G.K. Batchelor and A.A. Townsend (1949) showed that the non-Gaussian behavior of the probability density of dissipation quantities increases with decreasing scale. In a complementary sense, dissipation quantities become increasingly non-Gaussian as the Reynolds number increases. These are the two hallmarks of dissipation-scale intermittency. The scaling exponents for the energy dissipation are defined as

$$\langle\epsilon_r^q\rangle\,\langle\epsilon\rangle \propto (r/L)^{-\nu_q}. \tag{7.27}$$

The proportionality constants, omitted here, are not expected to be universal. The rationale for writing this power law can be explained in terms of the so-called breakdown coefficients or multipliers, which are supposed to represent the fractions in which the energy dissipation is shared when an eddy of size r is broken into two eddies, say, of size $r/2$. It is not clear that the multipliers, although quite useful, are fundamental to turbulence. Nontrivial scaling implies that ν_q is a nonlinear function of q. Indeed, there exist a broad class of models that attempt to explain the observed intermittency of the dissipative and inertial scales. These models are cast best in terms of multifractals (see *M.S. Borgas* (1992) for a summary), which provide a

convenient superstructure. *Kolmogorov's* original model is a degenerate case, as are other later models described by *A.S. Monin and A.M. Yaglom* (1975). The connection of these models to the Navier–Stokes equations is tenuous, and since the detailed physics of the models cannot be tested directly, their success should be evaluated chiefly on the basis of how well they agree with experiments.

Several efforts have been made to measure the exponents ν_q in (7.27), in both high and low Reynolds number flows. Given the difficulties in measuring them, the agreement among various data sets is surprisingly good.

Some other measures of the dissipation range intermittency include the scaling exponents for vorticity and circulation. The conclusion is that enstrophy is more intermittent than the energy dissipation rate. Similarly, the dissipation rate exponents for the passive scalar appear to also be more intermittent than the energy dissipation field in the inertial–convective range (between L and l_k). By contrast, in the viscous–convective range, it has been found that the scaling exponents are trivial (that is, there is no intermittency, and all intermittency exponents are essentially zero).

Computation of Turbulent Flows

Computing power has increased exponentially with time in the last few decades. One can in principle start with suitable initial conditions and compute the evolution of a turbulent flow by solving the Navier–Stokes equations without any further physical approximations. These are called direct numerical simulations (DNS) (see, e.g., *P. Moin, K. Mahesh* 1998). The hope is that it will be possible to compute many of the important flows by DNS, though it is clear that some others, such as the flow around an entire aircraft or ship, or in the ocean and the atmosphere, will remain out of bounds for many years to come, if they ever become amenable to direct numerical simulations. Thus, some inventiveness in our ability to calculate flows will be needed. It is also clear that the physics of turbulence cannot be understood merely by computing, though that step will help immensely if combined with organizing principles of the sort illustrated in this chapter. In one sense, we are still in the early stages of organization of our knowledge of turbulence. Vortex methods (see, e.g., *A.J. Chorin* (1994)), based on the representation of the turbulence by means of the vorticity field, offer an alternative in some cases, especially in two dimensions.

On the other end of the spectrum, since we are interested quite often in the mean characteristics of turbulent flow, one can write down the Reynolds equations for the mean quantities of interest by averaging the Navier–Stokes equations. It is clear from the discussion of Section 7.3 that additional terms will appear (see Section 5.2.2). For the equations describing the mean velocity these terms are the standard Reynolds stress terms, which need to be modeled suitably. This aspect of research has been important in practice, and is

motivated by the need to adapt our partial understanding of turbulence dynamics to obtain predictions of acceptable accuracy in engineering problems. One account of these models can be found in *C.G. Speziale* (1991).

In between these two extremes lies the scheme that computes only the large scale with temporal and spatial detail, while not resolving the small scales. The notion is that the large scales give shape to a flow and carry larger share of burden in the transport of heat, mass, and momentum, while the effects of the unresolved small scales, which need not be known in detail for most purposes, can be modeled by suitable parameterization. A sensible modeling of small scales is in principle attainable because of their nearly universal properties. This scheme of computation is known as large eddy simulations (or LES) of turbulence. Here, one writes down the equations for large scales only, and models the new terms that appear, these terms being similar to the Reynolds stress terms in the mean flow equations. Part of the reason for studying small-scale structure is indeed the understanding of its universal properties, so it can be suitably modeled and parameterized, thus allowing the computation of the large scale correctly. For reviews of these methods, see *M. Lesieur, O. Metais* (1996) and *S.B. Pope* (2000).

In recent years, a numerical scheme based on microscopic models and mesoscopic kinetic equations has been successfully employed to compute several turbulent flows. The models are based on what is now called the lattice Boltzmann methods (LBM). In conventional computational methods of fluid dynamics, one discretizes the macroscopic continuum equations on a suitably defined fine mesh before solving them. In LBM, on the other hand, one constructs simplified microscopic models that incorporate the essential physics, the basic premise being that the macroscopic dynamics, which are the result of a collective behavior of microscopic particles, are insensitive to the precise details of the microscopic physics, as long as one satisfies certain conservation properties. These methods are particularly suitable for fluid flows involving interfacial dynamics and complex boundaries. A summary of the methods can be found in *S. Chen, G.D. Doolen*, (1998).

7.5.1 Lagrangian Investigations of Turbulence

Since the transport properties of turbulence are dominated by the advection of infinitesimal fluid elements, it is natural to resort to the Lagrangian viewpoint, following the motion of the fluid elements. Lagrangian stochastic models have become important for the prediction of turbulent mixing and dispersion, with a particular emphasis on reacting flows; see *S.B. Pope* (2000). Early theoretical development in Lagrangian methods has been summarized by *A.S. Monin and A.M. Yaglom* (1975), and an idea of the recent work can be had from *P.K. Yeung* (2002).

Among the activities currently being pursued, one of the important ones is the use of DNS data, obtained in the Eulerian frame, to construct Lagrangian trajectories and compute selected properties, including velocity, ac-

celeration, time scales, velocity gradients, dissipation of energy, properties of the scalar passively carried along Lagrangian trajectories, and so forth. Lagrangian concepts have been usefully employed in subgrid scale modeling. At a fundamental level, they have been used to solve aspects of a model for passive scalars (see next section), and also to study the influence of geometry on scaling considerations by following Lagrangian clusters. There is, of course, the thought that Lagrangian studies may be more natural for studying the properties of coherent structures in turbulence. Finally, using some clever experimental methods initially developed for data acquisition in high-energy physics, *G.A. Voth et al.* (1998) have measured Lagrangian acceleration of particles and shown that the distributions have tails that spread to many standard deviations.

7.5.2 Field-Theoretic Methods

The turbulence problem, more than once described as the last unsolved problem in classical physics, perhaps no longer appears to be as "exceptional" as it once did, for other important strong-coupling problems have since been faced in theoretical physics. Some of these, such as color confinement in quantum chromodynamics, are still with us. For others, such as critical phenomena in three spactial dimensions, the critical scaling exponents have been calculated successfully by several methods, although other nonuniversal quantities of significant interest, such as critical temperatures, cannot yet be readily calculated for physical systems found in nature or realized in laboratories.

It is only natural to attempt to use these methods, employed with some success in similar problems, to address the basic problem of nonlinear coupling among scales of turbulence. Unfortunately, none of these methods that enabled breakthrough successes in the theory of critical phenomena have yet yielded results of comparable significance in understanding or predicting turbulent flows. Nevertheless, considerable progress has been made, and the application of such methods to turbulence has yielded some important insights. In particular, the perturbative techniques have scored a significant success in calculating turbulent scaling exponents in a simplified model of a white-noise advected passive scalar (for a review, see *Falkovich et al.* 2001).

7.5.3 Outlook

Turbulence is perhaps the most complex form of motion that fluid flows take. It contains structures and strong fluctuations, one embedded in the other. Consideration of one, and the neglect of the other, does not provide a full picture valid in all instances.

We have implied that it is convenient to think of a scale separation between the large scales that provide the shape and form for a given turbulent flow and the dissipative small scales, and that the interaction between them is

weak. This feature renders the small scale nearly universal, and amenable to a study independent of too many details of the flow. However, this is merely a model of turbulence, whose elucidation has taken much work. Details are emerging slowly.

It is often said that each turbulent flow is different. The large scales are indeed different. There is a varying degree of coherence in the large-scale motion, depending on initial and boundary conditions. The effects of this coherence can (and should) be captured eventually by appropriate statistics, but it is not clear that the statistics one uses, and constructs for reasons of mathematical convenience, are necessarily best adopted for taking faithful account of this observed coherence.

Another remark often made is that turbulence has nothing to do with stability. It is indeed the case that the instability caused by linear disturbances of negligible amplitude plays very little role in maintaining a turbulent flow, but stability arguments have been used consistently (and often successfully) to describe the observed coherent structures. The nature of this instability remains unclear at present. However, it is clear that a good student of turbulence ought to be versed in different aspects of hydrodynamic stability, and the variety of structures that can be generated by this mechanism. Automatically and logically, this leads us to the next chapter.